

Synthesis and electrical properties of $\text{Ce}_{1-x}\text{Gd}_x\text{O}_{2-x/2}$ ($x = 0.05\text{--}0.3$) solid solutions prepared by a citrate–nitrate combustion method

Xibao Li^{a,*}, Zhijun Feng^a, Jinshan Lu^a, Fajun Wang^a, Mingshan Xue^a, Gangqin Shao^b

^a School of Materials Science and Engineering, Nanchang Hangkong University, Nanchang 330063, PR China

^b State Key Laboratory of Advanced Technology for Materials Synthesis & Processing, Wuhan University of Technology, Wuhan 430070, PR China

Received 18 November 2011; received in revised form 9 December 2011; accepted 10 December 2011

Available online 19 December 2011

Abstract

$\text{Ce}_{1-x}\text{Gd}_x\text{O}_{2-x/2}$ (GDC) powders with different Gd^{3+} contents ($x = 0.05\text{--}0.3$) were prepared by a simple citrate–nitrate combustion method. The influence of the Gd^{3+} doping content on the crystal structure and the electrical properties of GDC were examined. Many analysis techniques such as thermal analysis, X-ray diffraction, nitrogen adsorption analysis, scanning electron microscopy and AC impedance analysis were employed to characterize the GDC powders. The crystallization of the GDC solid solution occurred below 350 °C. The GDC powders calcined at 800 °C showed a typical cubic fluorite structure. The lattice parameter of GDC exhibited a linear relationship with the Gd^{3+} content. As compared with that sintered at other temperatures, the GDC pellet that sintered at 1300 °C had a high relative density of 97%, and showed finer microstructure. The conductivity of GDC was firstly increased and then decreased with the increase of the Gd^{3+} content. The sintered GDC sample with the Gd^{3+} content of 0.25 exhibited the highest conductivity of $1.27 \times 10^{-2} \text{ S cm}^{-1}$ at 600 °C.

© 2011 Elsevier Ltd and Techna Group S.r.l. All rights reserved.

Keywords: C. Electrical properties; SOFC; GDC; Citrate–nitrate; Combustion

1. Introduction

Rare earth doped ceria solid solution is the most interesting candidate for an electrolyte material of intermediate and low temperature solid oxide fuel cells (SOFCs). Recently, ceria-based solid solutions, such as Sm-doped Ceria (SDC) and Gd-doped Ceria (GDC), were frequently used as an electrolyte for intermediate and low temperature SOFCs [1–4], both due to their high ionic conductivity compared to yttria-stabilized zirconia (YSZ) and compatibility with high-performance electrode materials in the intermediate and low temperature range. Among the rare earth doped ceria solid solutions, GDC and SDC have the highest electrical conductivity since the ionic radius of Gd^{3+} (or Sm^{3+}) was close to the ionic radius of Ce^{4+} [5].

A number of techniques have been employed to prepare the GDC electrolyte material. Compared with the conventional solid-state reaction processes, preparing the GDC oxide by wet

chemical method allows the production of powders with better stoichiometric control and higher purity. Recently, citrate method has attracted much attention in preparing SOFCs material since ultrafine powder with high purity, high sintering activity can be obtained by the citrate method that has the advantages of low cost and high efficiency [6,7].

In the present work, a simple citrate–nitrate combustion method was used to prepare the GDC electrolyte. In this method, citrate plays dual roles of a fuel and a complexing agent, nitrate acts as an oxidant. So the citrate–nitrate process is a self-sustaining combustion process that is simple and speedy. And the combustion process produces the powders with nanometer size and high specific area. These powders exhibit unique properties required for the SOFCs electrolyte. Therefore, in this work, the GDC electrolyte was prepared by the citrate–nitrate combustion method and the electrical properties in sintered samples were studied.

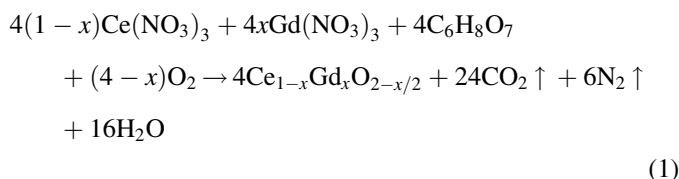
2. Experimental

$\text{Ce}_{1-x}\text{Gd}_x\text{O}_{2-x/2}$ ($x = 0.05\text{--}0.3$) was synthesized from metal nitrates and citric acid (brought from Sinopharm Chemical

* Corresponding author. Tel.: +86 791 86453203; fax: +86 791 86453203.

E-mail address: lixibao2007@yahoo.cn (X. Li).

Reagent Co., Ltd.). Cerium and gadolinium nitrate were dissolved in distilled water. Then these solutions were mixed by stoichiometric proportion. Citric acid was dissolved in distilled water and then was added into the cerium and gadolinium nitrate mixed solution. The mol ratio of citric acid to metal cation was adjusted to be 1:1. The mixed solution was stirred to remove excess water and then the transparent gel was formed in water-bath at 75 °C. The gel was heated and finally the thermal decomposition and combustion of the precursor happened instantly, and then the foam-like material was prepared. The reaction equation of the combustion reaction was shown in Eq. (1). The resulting foam-like material was then calcined at 800 °C for 2 h.



Thermal analysis (TG–DSC) of the GDC dried gel precursor was carried out in flowing air at a heating rate of 10 °C min^{−1} from room temperature to 1000 °C using a synchronous thermal analyzer (STA 449c/3/G, Netzsch, Germany). Specific surface area measurement was carried out by using nitrogen adsorption specific surface area analyzer (Gemini 2360 V5.00, Germany). Calcined powders were studied by XRD using a diffractometer (D/MAX-RB, Rigaku Corporation, Japan). SEM images were obtained by using a scanning electron microscope (JSM-5610LV, JEOL Ltd., Japan). The GDC powder was uniaxially pressed at 100 MPa to be formed in a 10 mm diameter pellets. The resulting green pellets were placed in a Pt crucible and sintered in air with a slow heating rate of 5 °C min^{−1}. Ag electrodes were deposited on both sides of the dense sintered GDC samples and fired at 800 °C for 1 h. AC impedance spectra (20 Hz–1 MHz) measurement was performed from room temperature to 600 °C in air by an electrochemical impedance spectrum analyzer (Model TH2818, Changzhou Tonghui Electronic Co. Ltd., China).

3. Results and discussion

3.1. Characterization of powders

In order to study the physical and chemical change, TG–DSC of the GDC gel precursor (after dried at 100 °C for 5 h) was carried out in flowing air from room temperature to 1000 °C. Fig. 1 shows the TG–DSC plot of the GDC gel precursor. From Fig. 1, it can be seen that the weight loss of the GDC gel precursor chiefly occurred below 350 °C. This meant that most physical and chemical changes occurred below 350 °C. The DSC curve exhibited three exothermic peaks that were around 162.2 °C, 221.4 °C and 306.1 °C, respectively. The exothermic peak around 162.2 °C could be ascribed to the combustion of the precursor, which was expressed in Eq. (1), for the theoretic weight loss of Eq. (1) (about 58–59%) was very close to the real weight loss of 58.02% that corresponding to the

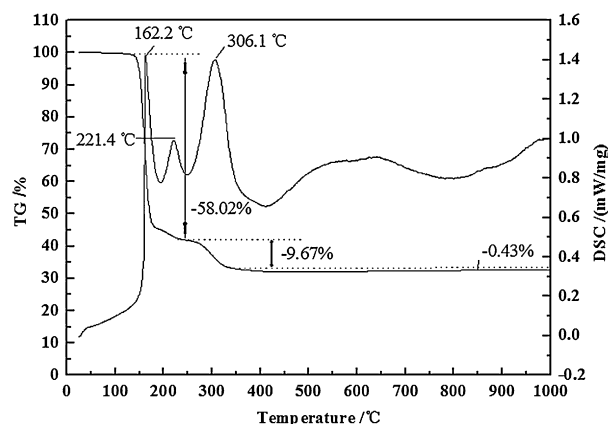


Fig. 1. TG–DSC plot of the GDC dried gel precursor.

exothermic peak around 162.2 °C. The one around 221.4 °C with a weight loss of about 9.67% could be related to the burnout of residual organic materials because citric acid was excessive in this system in order to guarantee the sufficient complexation of metallic ion. The one around 306.1 °C with no weight loss could be related to the crystallization of the GDC solid solution because the solution of Gd₂O₃ with CeO₂ was exothermic process and weight lossless. Furthermore, there exhibited an endothermic peak around 800 °C with a weight loss of 0.43% above 350 °C, which was likely to be ascribed to the divorce of oxygen from crystal lattice and the formation of oxygen vacancy that should be endothermic processes. So it was concluded that the crystallization of the GDC solid solution should occur below 350 °C.

X-ray diffraction patterns of self-made Ce_{1-x}Gd_xO_{2-x/2} ($x = 0.05$ – 0.3) powders and commercial pure CeO₂ (3.5 N) powder are shown in Fig. 2. These showed that all Ce_{1-x}Gd_xO_{2-x/2} ($x = 0.05$ – 0.3) solid solutions with different Gd³⁺ contents exhibited a cubic fluorite phase. And no impurity phase existed. These illustrated that Gd³⁺ was doped into the CeO₂ crystal lattice and the GDC solid solution was formed.

The lattice parameter (a) of Ce_{1-x}Gd_xO_{2-x/2} ($x = 0.05$ – 0.3) was calculated by software JADE 5.0. The relationship between the lattice parameter (a) of Ce_{1-x}Gd_xO_{2-x/2} ($x = 0.05$ – 0.3) and

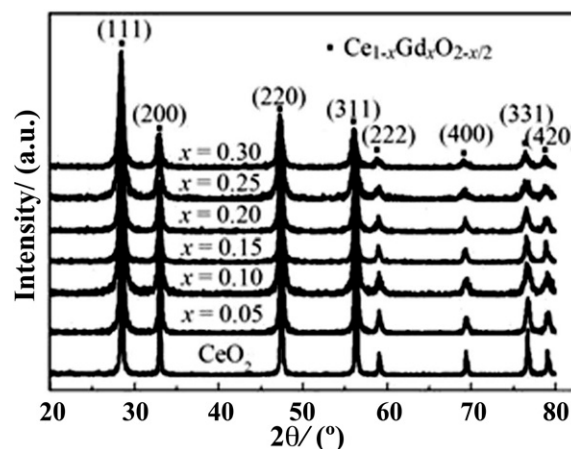


Fig. 2. XRD patterns of the GDC powders.

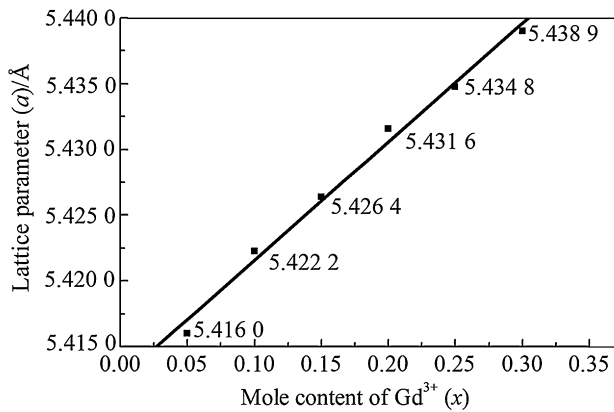


Fig. 3. Relationship between the lattice parameter (a) of GDC and the Gd^{3+} doping content (x).

the doping content (x) is shown in Fig. 3. It could be seen that the lattice parameter increased with the increase of the doping content. By a linear fitting, the relational expression of “ a ” and “ x ” was shown in Eq. (2).

$$a = 5.4126 + 0.0901x \quad (2)$$

The increase of the lattice parameter indicated an expansion of the unit cell of CeO_2 . Since the ionic radius of Gd^{3+} (0.1053 nm) was larger than the ionic radius of Ce^{4+} (0.097 nm). With the increase of the Gd^{3+} doping content, the unit cell of CeO_2 expanded. The solid solubility of Gd^{3+} in CeO_2 reached 30 mol% after GDC was calcined at 800 °C for 2 h.

The crystallite size (d) of the GDC powders was estimated by the Scherrer's formula:

$$d = \frac{0.9\lambda}{\beta \cos \theta} \quad (3)$$

where λ was the wavelength of the X-ray radiation (1.5418 Å), β was the full width of diffraction peak at half maximum and θ was the scattering angle of the main reflection (1 1 1). The average crystallite sizes were given in Table 1.

Specific surface area (A) and primary particle size (D) were calculated from the BET data of the GDC powders that calcined at 800 °C with different Gd^{3+} doping contents, which were also given in Table 1. These showed that the average crystallite sizes were 13–23 nm and the primary particle sizes were 22–36 nm.

Table 1
Average crystallite size (d), primary particle size (D) and specific surface area (A) of the GDC powders with different Gd^{3+} doping contents.

x	d (nm)	D (nm)	A ($\text{m}^2 \text{g}^{-1}$)
0.05	23	36	23.1035
0.10	14	22	38.4641
0.15	22	32	25.8374
0.20	19	29	29.0929
0.25	13	24	34.6388
0.30	15	27	30.7263

The crystallite sizes and the particle sizes of the GDC powders were very small and the specific surface areas of the GDC powders were considerable large, which indicated that the GDC powders had high sintering activity.

Otherwise, the crystallite size, the primary particle size and the specific surface area of the GDC powders exhibited no obvious relationships with the Gd^{3+} doping content. However, the crystallite size had a direct proportion to the particle size. The reason was likely to be that the primary particle was composed by the crystallite.

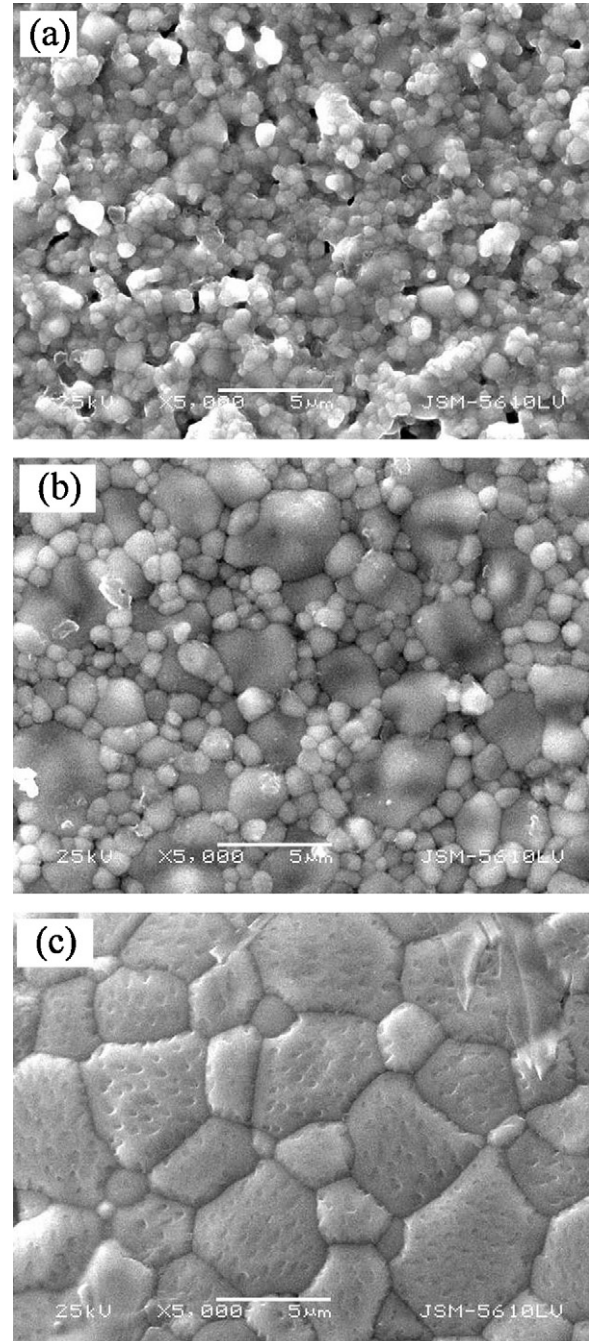


Fig. 4. SEM images of GDC sintered at (a) 1200 °C, (b) 1300 °C and (c) 1400 °C.

3.2. Sintering

The GDC powders were pressed and sintered at different temperatures. Fig. 4 illustrated the SEM images of GDC sintered at 1200–1400 °C for 2 h. From the morphology of GDC sintered at 1200 °C for 2 h (seen in Fig. 4(a)), it could be seen that there were some holes in it. The grains seemed to be very small and the grain boundary was not obvious. The GDC pellet sintered at this temperature was not compact, even loose to some extent. The relative density of GDC sintered at 1200 °C was only 88%. These indicated that GDC was underburnt at this temperature.

For the GDC pellet sintered at 1300 °C for 2 h, the relative density reached 97%. From Fig. 4(b) it could be seen that the microstructure was dense. The grains closely connected with each other and the grain boundary was very obvious. Most grains maintained to be fine. However, when the sintering temperature increased to 1400 °C, the grains grew up abnormally and the most of the grains became very large (seen in Fig. 4(c)). These showed that the GDC powders prepared by citrate–nitrate combustion method had high sintering activity, which led to the result that GDC was easy to be sintered to porcelain at relatively low temperature.

However, the GDC grains grew up from 500 to 1000 nm at the lowest sintering temperature, up to 5000 nm and higher at the highest sintering temperature. The dramatic increase of the particle sizes during sintering is due to the secondary recrystallization of grains, which can be attributed to the non-homogeneous primary particle and slow sintering rate.

3.3. Electrical properties

AC impedance spectra of the GDC pellet tested 300 °C, 400 °C, 500 °C and 600 °C was shown in Fig. 5. There should be high, intermediate and low characteristic frequencies corresponding to the bulk, grain boundary and electrode processes in the figures. However, there were not obvious high characteristic frequencies corresponding to the bulk resistance in the figures. The reason was that the high characteristic frequencies corresponding to the bulk resistance were generally 10^6 – 10^7 Hz. But AC impedance spectra test was performed at the frequencies of 20 Hz–1 MHz. With the temperature increasing from 300 °C to 600 °C, the semicircle arc corresponding to the grain boundary resistance shrank. As the temperature rose to 600 °C, there was only spike corresponding to the grain boundary resistance left. However, the semicircle arc corresponding to the electrode processes spread out with the temperature increasing from 300 °C to 600 °C. These illustrated that the electrical conduction of GDC was gradually controlled by the electrode processes with the temperature increased.

The Arrhenius plots of GDC's conductivity with different Gd^{3+} doping contents (x) were shown in Fig. 6. It could be seen that the conductivity exhibited Arrhenius behavior. With the Gd^{3+} doping content increasing from 0.05 to 0.25, the conductivity of the $\text{Ce}_{1-x}\text{Gd}_x\text{O}_{2-x/2}$ solid solutions increased and reached maximal value at $x = 0.25$. However, the conductivity decreased after the Gd^{3+} content was larger than 0.25. The reason was likely to be that the mean distance of

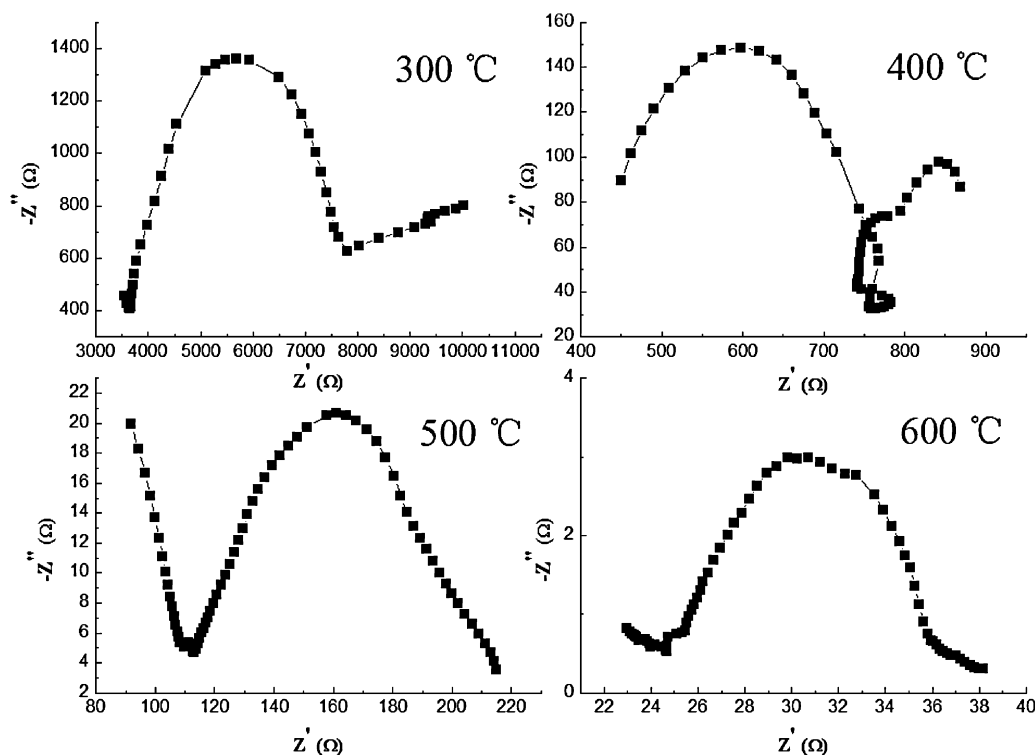


Fig. 5. Impedance spectra of GDC tested at different temperatures.

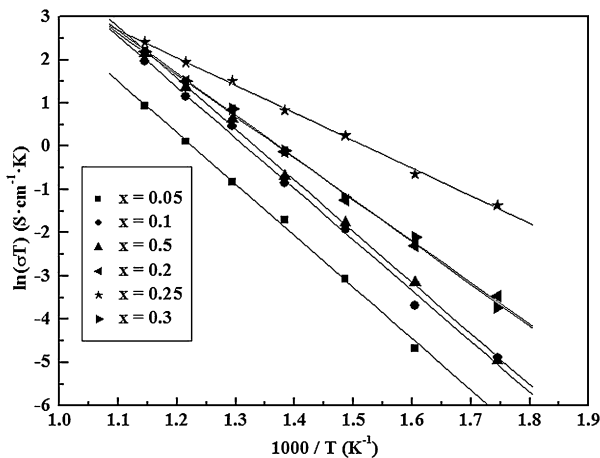


Fig. 6. Arrhenius plots of the conductivities of $\text{Ce}_{1-x}\text{Gd}_x\text{O}_{2-x/2}$ ($x = 0.05\text{--}0.3$).

Table 2

Compare of the electrical properties of GDC prepared by different methods.

Composition	Synthesis method	σ (10^{-2} S cm $^{-1}$)	Activation energy (eV)	Refs.
$\text{Ce}_{0.9}\text{Gd}_{0.1}\text{O}_{1.95}$	Co-precipitation	1.64	0.62	[8]
$\text{Ce}_{0.8}\text{Gd}_{0.2}\text{O}_{1.9}$	Modified pechini	0.98	1.04	[9]
$\text{Ce}_{0.9}\text{Gd}_{0.1}\text{O}_{1.95}$	EDTA–citrate	1.17	0.93	[10]
$\text{Ce}_{0.75}\text{Gd}_{0.25}\text{O}_{1.85}$	Citrate–nitrate	1.27	0.55	This work

($\text{Gd}'_{\text{Ce}} - \text{V}_{\text{O}}^{\bullet\bullet}$) defect complex was far, and the oxygen vacancy was bounded in the defect complex and difficult to migrate, which resulted in the low conductivity of GDC. With the increasing of the Gd^{3+} doping content, the mean distance of ($\text{Gd}'_{\text{Ce}} - \text{V}_{\text{O}}^{\bullet\bullet}$) defect complex became near even negative, the effective concentration and the transition probability of oxygen vacancy increased, which led to the gradual increase of the conductivity. However, with the further increasing of the Gd^{3+} doping content, the dual defects might compound, the effective concentration and the transition probability of oxygen vacancy decreased, which resulted in the reducing of the conductivity.

The highest conductivity value in this work was 1.27×10^{-2} S cm $^{-1}$, which was the conductivity value of GDC that tested at 600 °C with the Gd^{3+} doping content of 0.25. The corresponding activation energy for conduction that calculated from the line slope in Fig. 6 was 0.55 eV. These electrical property values were compared with the best values of GDC that synthesized by other methods at the same testing temperature, which were shown in Table 2. These showed that GDC prepared by the citrate–nitrate combustion method had preferable electrical properties.

4. Conclusions

A simple, speedy and effective citrate–nitrate combustion method was successfully used to prepare the nanometer GDC powders with the average crystallite sizes of 13–23 nm and the

primary particle sizes of 22–36 nm. The TG–DSC result showed that the crystallization of the GDC solid solution occurred below 350 °C. All $\text{Ce}_{1-x}\text{Gd}_x\text{O}_{2-x/2}$ ($x = 0.05\text{--}0.3$) solid solutions with different Gd^{3+} doping contents exhibited a cubic fluorite phase. The lattice parameter of GDC exhibited a linear relationship with the Gd^{3+} doping content. The GDC samples sintered at 1300 °C reached a relative density of 97% and showed relatively finer microstructure than those sintered at 1200 °C and 1400 °C. The sintered GDC samples were relatively denser and showed finer microstructure at relatively lower sintering temperature, which was due to the high specific area and sintering activity of GDC that prepared by the citrate–nitrate combustion method. With the increasing of the Gd^{3+} doping content, the conductivity of GDC was firstly increased and then decreased. At the Gd^{3+} doping content of 0.25, the GDC sample reached the highest conductivity value of 1.27×10^{-2} S cm $^{-1}$ with the activation energy for conduction of 0.55 eV.

Acknowledgements

The authors acknowledge the financial support from State Key Laboratory of Advanced Technology for Materials Synthesis and Processing (Wuhan University of Technology) (Grant No. 2012-KF-8), and from Research Foundation for Doctors of Nanchang Hangkong University (Grant No. EA201001197).

References

- [1] A. Gondolini, E. Mercadelli, A. Sanson, S. Albonetti, L. Doubova, S. Boldrini, Microwave-assisted synthesis of gadolinia-doped ceria powders for solid oxide fuel cells, *Ceram. Int.* 37 (2011) 1423–1426.
- [2] Y.P. Fu, Y.C. Liu, S.H. Hu, Aqueous tape casting and crystallization behavior of gadolinium-doped ceria, *Ceram. Int.* 35 (2009) 3153–3159.
- [3] M. Ana, L. Aitor, R. Lide, N.M. Luisa, P. Jose, L. Ander, A.M. Isabel, Chemical compatibility between YSZ and SDC sintered at different atmospheres for SOFC applications, *J. Power Sources* 192 (2009) 151–157.
- [4] Y.K. Tao, J. Shao, J.X. Wang, W.G. Wang, Morphology control of $\text{Ce}_{0.9}\text{Gd}_{0.1}\text{O}_{1.95}$ nanopowder synthesized by sol–gel method using PVP as a surfactant, *J. Alloys Compd.* 484 (2009) 729–733.
- [5] M. Mogensen, N.M. Sammes, G.A. Tompsett, Physical, chemical and electrochemical properties of pure and doped ceria, *Solid State Ionics* 129 (2000) 63–94.
- [6] R.O. Fuentes, R.T. Baker, Structural, morphological and electrical properties of $\text{Gd}_{0.1}\text{Ce}_{0.9}\text{O}_{1.95}$ prepared by a citrate complexation method, *J. Power Sources* 186 (2009) 268–277.
- [7] K.C. Patil, M.S. Hegde, T. Rattan, S.T. Aruna, Chemistry of nanocrystalline oxide materials, in: *Combustion Synthesis, Properties and Applications*, World Scientific, 2008, pp. 117–153.
- [8] P.D. Hari, H.R. Kim, J.S. Park, J.W. Son, B.K. Kim, H.W. Lee, J.H. Lee, Superior sinterability of nano-crystalline gadolinium doped ceria powders synthesized by co-precipitation method, *J. Alloys Compd.* 495 (2010) 238–241.
- [9] S. Molin, M. Gazda, P. Jasinski, Conductivity improvement of $\text{Ce}_{0.8}\text{Gd}_{0.2}\text{O}_{1.9}$ solid electrolyte, *J. Rare Earth* 27 (2009) 655–660.
- [10] R.R. Kondakindi, K. Karan, Characterization of Fe and Mn-doped GDC for low-temperature processing of solid oxide fuel cells, *Mater. Chem. Phys.* 115 (2009) 728–734.